

Supplement of Atmos. Chem. Phys., 15, 11291–11309, 2015
<http://www.atmos-chem-phys.net/15/11291/2015/>
doi:10.5194/acp-15-11291-2015-supplement
© Author(s) 2015. CC Attribution 3.0 License.



Supplement of

Advanced source apportionment of size-resolved trace elements at multiple sites in London during winter

S. Visser et al.

Correspondence to: J. G. Slowik (jay.slowik@psi.ch)

The copyright of individual parts of the supplement might differ from the CC-BY 3.0 licence.

Supplement

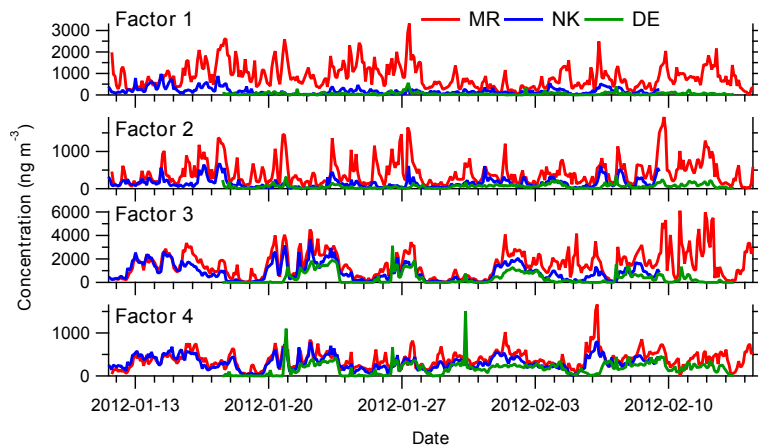


Figure 1. Non-optimal $PM_{10-2.5}$ source contributions (factor time series) with unconstrained ME-2 analysis on combined data of the three sites (MR - Marylebone Road, kerbside; NK - North Kensington, urban background; DE - Detling, rural). Factor 1 indicates mixed traffic-related and brake wear; factor 2 resuspended dust; factor 3 sea/road salt; factor 4 aged sea salt. See Fig. S4 for accompanying source profiles.

The residuals of Ni, Cr and Mo remain large at DE. Unconstrained ME-2 on five or six factors leads to unstable results varying strongly with seed. The dust factor splits in factors rich in Al and Si, and in Ca, but without improving residuals. A brake wear factor or a factor with Ni, Cr and Mo does not appear with increasing number of factors.

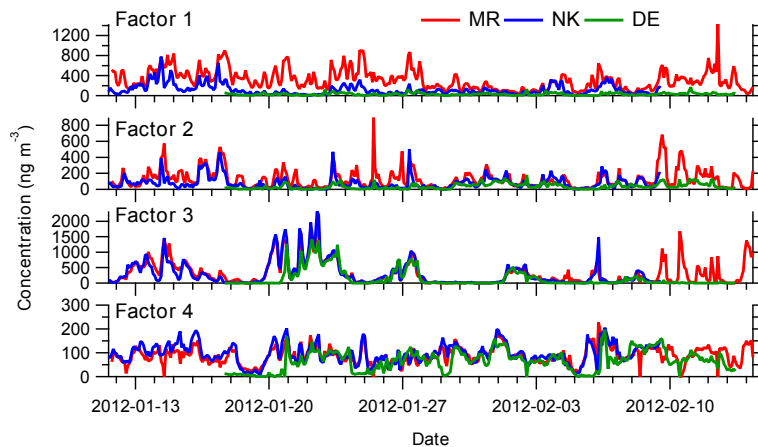


Figure 2. Non-optimal $PM_{2.5-1.0}$ source contributions (factor time series) with unconstrained ME-2 analysis on combined data of the three sites (MR - Marylebone Road, kerbside; NK - North Kensington, urban background; DE - Detling, rural). Factor 1 indicates mixed traffic-related and brake wear; factor 2 resuspended dust; factor 3 sea/road salt; factor 4 mixed aged sea salt and regional transport. See Fig. S4 for accompanying source profiles.

Unconstrained ME-2 on five or six factors leads to unstable results varying strongly with seed. The dust factor splits in factors rich in Al, and in Si and Ca, but without improving residuals. A brake wear factor does not appear with increasing number of factors. The factor containing mixed aged sea salt and regional transport cannot be unmixed in unconstrained ME-2.

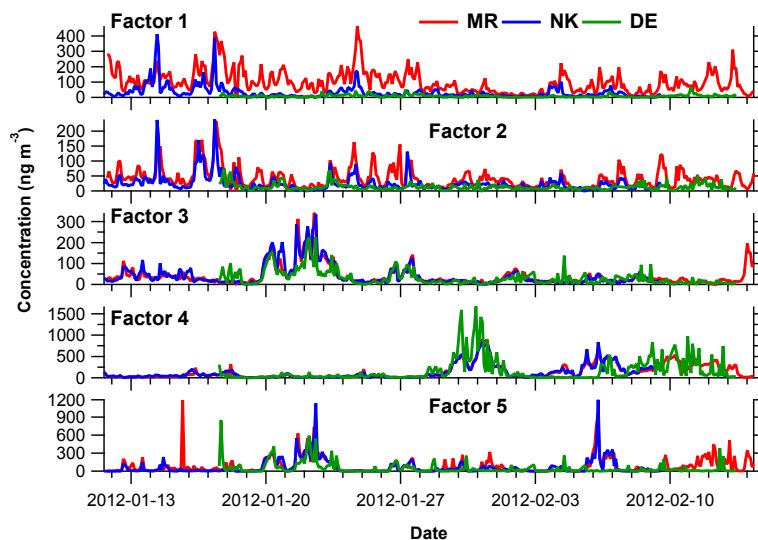


Figure 3. Non-optimal $PM_{1.0-0.3}$ source contributions (factor time series) with unconstrained ME-2 analysis on combined data of the three sites (MR - Marylebone Road, kerbside; NK - North Kensington, urban background; DE - Detling, rural). Factor 1 indicates traffic-related; factor 2 resuspended dust; factor 3 aged sea salt; factor 4 mixed S-rich and solid fuel; factor 5 mixed sea/road salt and Cl-rich. See Fig. S4 for accompanying source profiles.

Unconstrained ME-2 on six or seven factors leads to unstable results varying strongly with seed. The S-rich and solid fuel factor splits in a factor with only S as indicative for S-rich, but the second factor contains K without S. In a solid fuel source S can be expected. The mixed sea/road salt and Cl rich source (factor 5) is visible from the time series from roughly 20–24 January. This episode correlates strongly with factor 3 and with western wind, indicative of sea salt. Contrary, the episode from 5–7 February is absent in factor 3 and at the rural site, indicative of a source with fine Cl.

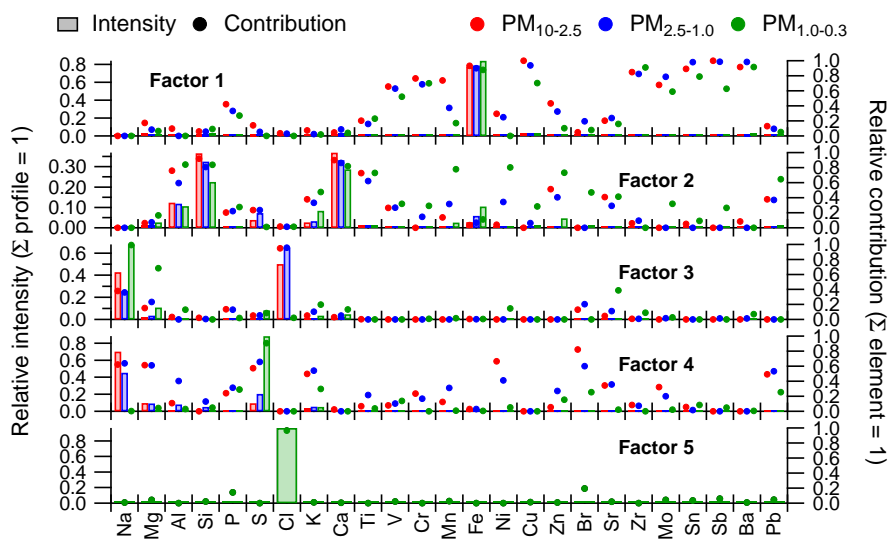


Figure 4. Non-optimal source profiles of unconstrained ME-2 analysis on combined data of the three sites (MR - Marylebone Road, kerbside; NK - North Kensington, urban background; DE - Detling, rural). The bars (left y-axis) represent the average element intensity to each factor in ng ng^{-1} , the circles (right y-axis) the fraction of the total predicted concentration for a given element. See Figs. S1–3 for an indication of the sources and why these profiles are considered non-optimal.

Table 1. Source profiles of ME-2 results on combined data of the MR-NK-DE sites for PM_{10-2.5} with mean ± 1 standard deviation (std) from the anchor sensitivity analysis. Relative intensity in ng ng⁻¹ represents the average element contribution to the factor (\sum profile = 1). Relative contribution denotes the fraction of the total predicted concentration for a given element (\sum contribution = 1). See also Fig. 3.

| Relative intensity | | | | | | | | | | | | | |
|-----------------------|------------|-------|---------|-------|-------|-------|---------------|-------|---------------|-------|------------|-------|--|
| Element | Brake wear | | Traffic | | Dust | | Sea/road salt | | Aged sea salt | | Industrial | | |
| | mean | std | mean | std | mean | std | mean | std | mean | std | mean | std | |
| Na | 0.000 | 0.000 | 0.000 | 0.000 | 0.000 | 0.000 | 0.434 | 0.013 | 0.668 | 0.009 | 0.000 | 0.000 | |
| Mg | 0.030 | 0.003 | 0.020 | 0.003 | 0.018 | 0.002 | 0.024 | 0.002 | 0.089 | 0.004 | 0.000 | 0.000 | |
| Al | 0.034 | 0.004 | 0.011 | 0.002 | 0.095 | 0.007 | 0.004 | 0.000 | 0.025 | 0.002 | 0.079 | 0.008 | |
| Si | 0.000 | 0.000 | 0.014 | 0.002 | 0.292 | 0.015 | 0.002 | 0.000 | 0.028 | 0.002 | 0.069 | 0.007 | |
| P | 0.016 | 0.002 | 0.006 | 0.001 | 0.004 | 0.000 | 0.002 | 0.000 | 0.003 | 0.000 | 0.007 | 0.001 | |
| S | 0.000 | 0.000 | 0.019 | 0.003 | 0.039 | 0.004 | 0.008 | 0.001 | 0.088 | 0.006 | 0.003 | 0.000 | |
| Cl | 0.000 | 0.000 | 0.009 | 0.001 | 0.068 | 0.006 | 0.512 | 0.020 | 0.000 | 0.000 | 0.000 | 0.000 | |
| K | 0.000 | 0.000 | 0.003 | 0.000 | 0.023 | 0.002 | 0.003 | 0.000 | 0.035 | 0.002 | 0.007 | 0.001 | |
| Ca | 0.000 | 0.000 | 0.005 | 0.001 | 0.290 | 0.020 | 0.002 | 0.000 | 0.052 | 0.004 | 0.000 | 0.000 | |
| Ti | 0.011 | 0.001 | 0.002 | 0.000 | 0.008 | 0.001 | 0.000 | 0.000 | 0.001 | 0.000 | 0.000 | 0.000 | |
| V | 0.014 | 0.002 | 0.001 | 0.000 | 0.001 | 0.000 | 0.000 | 0.000 | 0.000 | 0.000 | 0.001 | 0.000 | |
| Cr | 0.019 | 0.002 | 0.004 | 0.001 | 0.001 | 0.000 | 0.000 | 0.000 | 0.000 | 0.000 | 0.381 | 0.029 | |
| Mn | 0.000 | 0.000 | 0.012 | 0.002 | 0.003 | 0.000 | 0.000 | 0.000 | 0.001 | 0.000 | 0.030 | 0.004 | |
| Fe | 0.000 | 0.000 | 0.890 | 0.016 | 0.143 | 0.012 | 0.008 | 0.001 | 0.000 | 0.000 | 0.000 | 0.000 | |
| Ni | 0.007 | 0.001 | 0.000 | 0.000 | 0.000 | 0.000 | 0.000 | 0.000 | 0.000 | 0.000 | 0.318 | 0.027 | |
| Cu | 0.360 | 0.028 | 0.002 | 0.000 | 0.003 | 0.000 | 0.000 | 0.000 | 0.000 | 0.000 | 0.003 | 0.000 | |
| Zn | 0.090 | 0.010 | 0.000 | 0.000 | 0.007 | 0.001 | 0.000 | 0.000 | 0.001 | 0.000 | 0.027 | 0.003 | |
| Br | 0.000 | 0.000 | 0.000 | 0.000 | 0.000 | 0.000 | 0.001 | 0.000 | 0.003 | 0.000 | 0.007 | 0.001 | |
| Sr | 0.007 | 0.001 | 0.000 | 0.000 | 0.001 | 0.000 | 0.000 | 0.000 | 0.001 | 0.000 | 0.002 | 0.000 | |
| Zr | 0.017 | 0.002 | 0.001 | 0.000 | 0.001 | 0.000 | 0.000 | 0.000 | 0.000 | 0.000 | 0.000 | 0.000 | |
| Mo | 0.033 | 0.004 | 0.000 | 0.000 | 0.000 | 0.000 | 0.000 | 0.000 | 0.001 | 0.000 | 0.053 | 0.006 | |
| Sn | 0.048 | 0.006 | 0.001 | 0.000 | 0.001 | 0.000 | 0.000 | 0.000 | 0.000 | 0.000 | 0.007 | 0.001 | |
| Sb | 0.051 | 0.006 | 0.000 | 0.000 | 0.000 | 0.000 | 0.000 | 0.000 | 0.000 | 0.000 | 0.004 | 0.000 | |
| Ba | 0.264 | 0.024 | 0.000 | 0.000 | 0.002 | 0.000 | 0.000 | 0.000 | 0.000 | 0.000 | 0.000 | 0.000 | |
| Pb | 0.000 | 0.000 | 0.000 | 0.000 | 0.001 | 0.000 | 0.000 | 0.000 | 0.002 | 0.000 | 0.001 | 0.000 | |
| Relative contribution | | | | | | | | | | | | | |
| Element | Brake wear | | Traffic | | Dust | | Sea/road salt | | Aged sea salt | | Industrial | | |
| | mean | std | mean | std | mean | std | mean | std | mean | std | mean | std | |
| Na | 0.000 | 0.000 | 0.000 | 0.000 | 0.000 | 0.000 | 0.394 | 0.007 | 0.606 | 0.007 | 0.000 | 0.000 | |
| Mg | 0.164 | 0.013 | 0.112 | 0.011 | 0.101 | 0.007 | 0.130 | 0.009 | 0.493 | 0.014 | 0.000 | 0.000 | |
| Al | 0.137 | 0.011 | 0.043 | 0.005 | 0.383 | 0.017 | 0.015 | 0.001 | 0.101 | 0.006 | 0.321 | 0.019 | |
| Si | 0.000 | 0.000 | 0.035 | 0.004 | 0.721 | 0.015 | 0.004 | 0.000 | 0.070 | 0.005 | 0.170 | 0.014 | |
| P | 0.431 | 0.025 | 0.153 | 0.017 | 0.097 | 0.008 | 0.058 | 0.005 | 0.083 | 0.005 | 0.179 | 0.016 | |
| S | 0.000 | 0.000 | 0.117 | 0.017 | 0.250 | 0.022 | 0.052 | 0.006 | 0.560 | 0.026 | 0.021 | 0.003 | |
| Cl | 0.000 | 0.000 | 0.015 | 0.003 | 0.116 | 0.012 | 0.869 | 0.013 | 0.000 | 0.000 | 0.000 | 0.000 | |
| K | 0.000 | 0.000 | 0.042 | 0.008 | 0.320 | 0.030 | 0.046 | 0.006 | 0.495 | 0.032 | 0.097 | 0.014 | |
| Ca | 0.000 | 0.000 | 0.014 | 0.003 | 0.831 | 0.015 | 0.005 | 0.001 | 0.149 | 0.014 | 0.000 | 0.000 | |
| Ti | 0.515 | 0.039 | 0.080 | 0.014 | 0.344 | 0.034 | 0.000 | 0.000 | 0.062 | 0.006 | 0.000 | 0.000 | |
| V | 0.818 | 0.021 | 0.067 | 0.012 | 0.056 | 0.007 | 0.000 | 0.000 | 0.017 | 0.002 | 0.042 | 0.007 | |
| Cr | 0.046 | 0.007 | 0.010 | 0.002 | 0.002 | 0.000 | 0.000 | 0.000 | 0.001 | 0.000 | 0.941 | 0.008 | |
| Mn | 0.002 | 0.000 | 0.255 | 0.038 | 0.070 | 0.009 | 0.000 | 0.000 | 0.015 | 0.002 | 0.658 | 0.040 | |
| Fe | 0.000 | 0.000 | 0.855 | 0.012 | 0.137 | 0.012 | 0.007 | 0.001 | 0.000 | 0.000 | 0.000 | 0.000 | |
| Ni | 0.022 | 0.004 | 0.001 | 0.000 | 0.001 | 0.000 | 0.000 | 0.000 | 0.001 | 0.000 | 0.975 | 0.004 | |
| Cu | 0.975 | 0.002 | 0.006 | 0.001 | 0.009 | 0.001 | 0.001 | 0.000 | 0.000 | 0.000 | 0.009 | 0.001 | |
| Zn | 0.717 | 0.030 | 0.003 | 0.000 | 0.058 | 0.007 | 0.000 | 0.000 | 0.008 | 0.001 | 0.214 | 0.028 | |
| Br | 0.000 | 0.000 | 0.017 | 0.004 | 0.000 | 0.000 | 0.053 | 0.007 | 0.285 | 0.029 | 0.645 | 0.033 | |
| Sr | 0.664 | 0.033 | 0.000 | 0.000 | 0.053 | 0.007 | 0.011 | 0.001 | 0.063 | 0.006 | 0.210 | 0.028 | |
| Zr | 0.902 | 0.012 | 0.047 | 0.009 | 0.029 | 0.004 | 0.001 | 0.000 | 0.021 | 0.002 | 0.000 | 0.000 | |
| Mo | 0.377 | 0.041 | 0.004 | 0.001 | 0.006 | 0.001 | 0.000 | 0.000 | 0.008 | 0.001 | 0.605 | 0.042 | |
| Sn | 0.838 | 0.022 | 0.009 | 0.002 | 0.013 | 0.002 | 0.000 | 0.000 | 0.008 | 0.001 | 0.131 | 0.020 | |
| Sb | 0.926 | 0.012 | 0.001 | 0.000 | 0.000 | 0.000 | 0.001 | 0.000 | 0.000 | 0.000 | 0.071 | 0.012 | |
| Ba | 0.991 | 0.001 | 0.000 | 0.000 | 0.007 | 0.001 | 0.001 | 0.000 | 0.000 | 0.000 | 0.000 | 0.000 | |
| Pb | 0.000 | 0.000 | 0.106 | 0.020 | 0.238 | 0.027 | 0.000 | 0.000 | 0.356 | 0.030 | 0.300 | 0.036 | |

Table 2. Source profiles of ME-2 results on combined data of the MR-NK-DE sites for PM_{2.5-1.0} with mean \pm 1 standard deviation (std) from the anchor sensitivity analysis. Relative intensity in ng ng⁻¹ represents the average element contribution to the factor (\sum profile = 1). Relative contribution denotes the fraction of the total predicted concentration for a given element (\sum contribution = 1). See also Fig. 3.

| Relative intensity | | | | | | | | | | | | |
|-----------------------|------------|-------|---------|-------|-------|-------|---------------|-------|---------------|-------|--------|-------|
| Element | Brake wear | | Traffic | | Dust | | Sea/road salt | | Aged sea salt | | S-rich | |
| | mean | std | mean | std | mean | std | mean | std | mean | std | mean | std |
| Na | 0.000 | 0.000 | 0.000 | 0.000 | 0.000 | 0.000 | 0.225 | 0.010 | 0.640 | 0.005 | 0.000 | 0.000 |
| Mg | 0.021 | 0.002 | 0.012 | 0.002 | 0.007 | 0.001 | 0.033 | 0.002 | 0.100 | 0.003 | 0.050 | 0.004 |
| Al | 0.034 | 0.004 | 0.011 | 0.001 | 0.089 | 0.006 | 0.000 | 0.000 | 0.067 | 0.003 | 0.005 | 0.000 |
| Si | 0.000 | 0.000 | 0.038 | 0.005 | 0.284 | 0.013 | 0.005 | 0.000 | 0.028 | 0.001 | 0.038 | 0.003 |
| P | 0.017 | 0.002 | 0.006 | 0.001 | 0.005 | 0.000 | 0.003 | 0.000 | 0.005 | 0.000 | 0.009 | 0.001 |
| S | 0.000 | 0.000 | 0.001 | 0.000 | 0.005 | 0.000 | 0.027 | 0.002 | 0.085 | 0.004 | 0.576 | 0.020 |
| Cl | 0.000 | 0.000 | 0.020 | 0.003 | 0.000 | 0.000 | 0.672 | 0.025 | 0.000 | 0.000 | 0.036 | 0.003 |
| K | 0.000 | 0.000 | 0.003 | 0.000 | 0.020 | 0.002 | 0.010 | 0.001 | 0.046 | 0.002 | 0.058 | 0.005 |
| Ca | 0.000 | 0.000 | 0.040 | 0.005 | 0.300 | 0.020 | 0.020 | 0.001 | 0.000 | 0.000 | 0.014 | 0.001 |
| Ti | 0.012 | 0.001 | 0.003 | 0.000 | 0.009 | 0.001 | 0.000 | 0.000 | 0.003 | 0.000 | 0.004 | 0.000 |
| V | 0.014 | 0.002 | 0.002 | 0.000 | 0.001 | 0.000 | 0.000 | 0.000 | 0.000 | 0.000 | 0.001 | 0.000 |
| Cr | 0.019 | 0.002 | 0.004 | 0.001 | 0.002 | 0.000 | 0.000 | 0.000 | 0.000 | 0.000 | 0.000 | 0.000 |
| Mn | 0.000 | 0.000 | 0.010 | 0.001 | 0.007 | 0.001 | 0.000 | 0.000 | 0.005 | 0.000 | 0.000 | 0.000 |
| Fe | 0.000 | 0.000 | 0.820 | 0.023 | 0.252 | 0.020 | 0.003 | 0.000 | 0.014 | 0.001 | 0.170 | 0.015 |
| Ni | 0.007 | 0.001 | 0.000 | 0.000 | 0.000 | 0.000 | 0.000 | 0.000 | 0.000 | 0.000 | 0.001 | 0.000 |
| Cu | 0.332 | 0.027 | 0.011 | 0.002 | 0.005 | 0.000 | 0.000 | 0.000 | 0.000 | 0.000 | 0.007 | 0.001 |
| Zn | 0.092 | 0.010 | 0.003 | 0.000 | 0.007 | 0.001 | 0.000 | 0.000 | 0.002 | 0.000 | 0.014 | 0.001 |
| Br | 0.000 | 0.000 | 0.001 | 0.000 | 0.000 | 0.000 | 0.001 | 0.000 | 0.001 | 0.000 | 0.005 | 0.001 |
| Sr | 0.009 | 0.001 | 0.000 | 0.000 | 0.001 | 0.000 | 0.000 | 0.000 | 0.001 | 0.000 | 0.001 | 0.000 |
| Zr | 0.018 | 0.002 | 0.002 | 0.000 | 0.001 | 0.000 | 0.000 | 0.000 | 0.001 | 0.000 | 0.000 | 0.000 |
| Mo | 0.034 | 0.004 | 0.002 | 0.000 | 0.000 | 0.000 | 0.000 | 0.000 | 0.000 | 0.000 | 0.001 | 0.000 |
| Sn | 0.049 | 0.005 | 0.003 | 0.000 | 0.001 | 0.000 | 0.000 | 0.000 | 0.000 | 0.000 | 0.001 | 0.000 |
| Sb | 0.052 | 0.006 | 0.001 | 0.000 | 0.000 | 0.000 | 0.000 | 0.000 | 0.000 | 0.000 | 0.000 | 0.000 |
| Ba | 0.290 | 0.025 | 0.008 | 0.001 | 0.003 | 0.000 | 0.001 | 0.000 | 0.000 | 0.000 | 0.003 | 0.000 |
| Pb | 0.000 | 0.000 | 0.001 | 0.000 | 0.002 | 0.000 | 0.000 | 0.000 | 0.001 | 0.000 | 0.005 | 0.000 |
| Relative contribution | | | | | | | | | | | | |
| Element | Brake wear | | Traffic | | Dust | | Sea/road salt | | Aged sea salt | | S-rich | |
| | mean | std | mean | std | mean | std | mean | std | mean | std | mean | std |
| Na | 0.000 | 0.000 | 0.000 | 0.000 | 0.000 | 0.000 | 0.260 | 0.006 | 0.740 | 0.006 | 0.000 | 0.000 |
| Mg | 0.096 | 0.007 | 0.053 | 0.005 | 0.032 | 0.002 | 0.148 | 0.007 | 0.447 | 0.009 | 0.225 | 0.011 |
| Al | 0.164 | 0.012 | 0.052 | 0.005 | 0.435 | 0.014 | 0.000 | 0.000 | 0.326 | 0.011 | 0.022 | 0.002 |
| Si | 0.000 | 0.000 | 0.097 | 0.009 | 0.722 | 0.011 | 0.013 | 0.001 | 0.072 | 0.003 | 0.096 | 0.007 |
| P | 0.384 | 0.022 | 0.140 | 0.014 | 0.102 | 0.008 | 0.063 | 0.004 | 0.108 | 0.005 | 0.203 | 0.015 |
| S | 0.000 | 0.000 | 0.002 | 0.000 | 0.007 | 0.001 | 0.039 | 0.003 | 0.123 | 0.006 | 0.829 | 0.007 |
| Cl | 0.000 | 0.000 | 0.027 | 0.005 | 0.000 | 0.000 | 0.923 | 0.008 | 0.000 | 0.000 | 0.050 | 0.006 |
| K | 0.000 | 0.000 | 0.020 | 0.004 | 0.147 | 0.019 | 0.075 | 0.009 | 0.332 | 0.022 | 0.426 | 0.031 |
| Ca | 0.000 | 0.000 | 0.106 | 0.016 | 0.803 | 0.019 | 0.053 | 0.005 | 0.000 | 0.000 | 0.037 | 0.005 |
| Ti | 0.385 | 0.037 | 0.087 | 0.016 | 0.308 | 0.031 | 0.000 | 0.000 | 0.086 | 0.006 | 0.133 | 0.017 |
| V | 0.769 | 0.025 | 0.086 | 0.015 | 0.061 | 0.008 | 0.001 | 0.000 | 0.004 | 0.000 | 0.079 | 0.010 |
| Cr | 0.748 | 0.030 | 0.159 | 0.026 | 0.061 | 0.008 | 0.000 | 0.000 | 0.019 | 0.001 | 0.014 | 0.002 |
| Mn | 0.004 | 0.001 | 0.450 | 0.043 | 0.306 | 0.038 | 0.000 | 0.000 | 0.239 | 0.019 | 0.000 | 0.000 |
| Fe | 0.000 | 0.000 | 0.651 | 0.017 | 0.200 | 0.016 | 0.002 | 0.000 | 0.011 | 0.001 | 0.135 | 0.013 |
| Ni | 0.808 | 0.021 | 0.041 | 0.008 | 0.042 | 0.005 | 0.000 | 0.000 | 0.000 | 0.000 | 0.109 | 0.014 |
| Cu | 0.933 | 0.007 | 0.032 | 0.005 | 0.015 | 0.002 | 0.001 | 0.000 | 0.000 | 0.000 | 0.020 | 0.002 |
| Zn | 0.781 | 0.021 | 0.022 | 0.004 | 0.058 | 0.008 | 0.000 | 0.000 | 0.017 | 0.001 | 0.122 | 0.015 |
| Br | 0.000 | 0.000 | 0.084 | 0.020 | 0.000 | 0.000 | 0.122 | 0.016 | 0.155 | 0.014 | 0.638 | 0.034 |
| Sr | 0.767 | 0.020 | 0.012 | 0.002 | 0.051 | 0.007 | 0.026 | 0.003 | 0.064 | 0.005 | 0.080 | 0.011 |
| Zr | 0.825 | 0.020 | 0.098 | 0.017 | 0.040 | 0.005 | 0.000 | 0.000 | 0.038 | 0.003 | 0.000 | 0.000 |
| Mo | 0.895 | 0.013 | 0.053 | 0.010 | 0.011 | 0.002 | 0.004 | 0.000 | 0.011 | 0.001 | 0.026 | 0.004 |
| Sn | 0.922 | 0.011 | 0.052 | 0.010 | 0.010 | 0.001 | 0.002 | 0.000 | 0.000 | 0.000 | 0.014 | 0.002 |
| Sb | 0.968 | 0.005 | 0.024 | 0.005 | 0.005 | 0.001 | 0.003 | 0.000 | 0.000 | 0.000 | 0.000 | 0.000 |
| Ba | 0.955 | 0.005 | 0.025 | 0.004 | 0.008 | 0.001 | 0.003 | 0.000 | 0.000 | 0.000 | 0.009 | 0.001 |
| Pb | 0.000 | 0.000 | 0.083 | 0.018 | 0.191 | 0.027 | 0.000 | 0.000 | 0.169 | 0.015 | 0.557 | 0.039 |

Table 3. Source profiles of ME-2 results on combined data of the MR-NK-DE sites for PM_{1.0-0.3} with mean ± 1 standard deviation (std) from the anchor sensitivity analysis. Relative intensity in ng ng⁻¹ represents the average element contribution to the factor (\sum profile = 1). Relative contribution denotes the fraction of the total predicted concentration for a given element (\sum contribution = 1). See also Fig. 3.

| Relative intensity | | | | | | | | | | | | | | |
|-----------------------|---------|-------|-------|-------|---------------|-------|---------------|-------|--------|-------|------------|-------|------------|-------|
| Element | Traffic | | Dust | | Sea/road salt | | Aged sea salt | | S-rich | | Solid fuel | | Reacted Cl | |
| | mean | std | mean | std | mean | std | mean | std | mean | std | mean | std | mean | std |
| Na | 0.000 | 0.000 | 0.000 | 0.000 | 0.223 | 0.005 | 0.705 | 0.004 | 0.000 | 0.000 | 0.000 | 0.000 | 0.000 | 0.000 |
| Mg | 0.011 | 0.002 | 0.013 | 0.001 | 0.033 | 0.002 | 0.147 | 0.005 | 0.004 | 0.000 | 0.013 | 0.001 | 0.010 | 0.001 |
| Al | 0.004 | 0.001 | 0.084 | 0.007 | 0.001 | 0.000 | 0.055 | 0.002 | 0.005 | 0.000 | 0.000 | 0.000 | 0.002 | 0.000 |
| Si | 0.020 | 0.003 | 0.240 | 0.014 | 0.003 | 0.000 | 0.005 | 0.000 | 0.013 | 0.001 | 0.035 | 0.003 | 0.004 | 0.000 |
| P | 0.008 | 0.001 | 0.006 | 0.000 | 0.003 | 0.000 | 0.000 | 0.000 | 0.008 | 0.001 | 0.013 | 0.001 | 0.004 | 0.000 |
| S | 0.000 | 0.000 | 0.001 | 0.000 | 0.043 | 0.003 | 0.000 | 0.000 | 0.949 | 0.004 | 0.463 | 0.022 | 0.000 | 0.000 |
| Cl | 0.000 | 0.000 | 0.000 | 0.000 | 0.659 | 0.017 | 0.000 | 0.000 | 0.000 | 0.000 | 0.000 | 0.000 | 0.964 | 0.004 |
| K | 0.000 | 0.000 | 0.000 | 0.000 | 0.012 | 0.001 | 0.047 | 0.002 | 0.000 | 0.000 | 0.312 | 0.022 | 0.008 | 0.001 |
| Ca | 0.011 | 0.002 | 0.346 | 0.022 | 0.019 | 0.001 | 0.029 | 0.001 | 0.001 | 0.000 | 0.000 | 0.000 | 0.000 | 0.000 |
| Ti | 0.003 | 0.000 | 0.010 | 0.001 | 0.000 | 0.000 | 0.000 | 0.000 | 0.000 | 0.000 | 0.003 | 0.000 | 0.000 | 0.000 |
| V | 0.003 | 0.000 | 0.001 | 0.000 | 0.000 | 0.000 | 0.000 | 0.000 | 0.000 | 0.000 | 0.001 | 0.000 | 0.000 | 0.000 |
| Cr | 0.005 | 0.001 | 0.002 | 0.000 | 0.000 | 0.000 | 0.000 | 0.000 | 0.000 | 0.000 | 0.000 | 0.000 | 0.000 | 0.000 |
| Mn | 0.011 | 0.002 | 0.012 | 0.001 | 0.001 | 0.000 | 0.001 | 0.000 | 0.000 | 0.000 | 0.005 | 0.000 | 0.000 | 0.000 |
| Fe | 0.836 | 0.020 | 0.246 | 0.019 | 0.000 | 0.000 | 0.000 | 0.000 | 0.005 | 0.001 | 0.048 | 0.004 | 0.001 | 0.000 |
| Ni | 0.001 | 0.000 | 0.001 | 0.000 | 0.001 | 0.000 | 0.000 | 0.000 | 0.000 | 0.000 | 0.000 | 0.000 | 0.000 | 0.000 |
| Cu | 0.029 | 0.004 | 0.010 | 0.001 | 0.000 | 0.000 | 0.000 | 0.000 | 0.000 | 0.000 | 0.002 | 0.000 | 0.000 | 0.000 |
| Zn | 0.009 | 0.001 | 0.020 | 0.002 | 0.000 | 0.000 | 0.000 | 0.000 | 0.001 | 0.000 | 0.064 | 0.006 | 0.000 | 0.000 |
| Br | 0.003 | 0.000 | 0.000 | 0.000 | 0.001 | 0.000 | 0.000 | 0.000 | 0.007 | 0.001 | 0.011 | 0.001 | 0.004 | 0.000 |
| Sr | 0.001 | 0.000 | 0.001 | 0.000 | 0.000 | 0.000 | 0.002 | 0.000 | 0.000 | 0.000 | 0.000 | 0.000 | 0.000 | 0.000 |
| Zr | 0.004 | 0.001 | 0.000 | 0.000 | 0.000 | 0.000 | 0.001 | 0.000 | 0.000 | 0.000 | 0.000 | 0.000 | 0.000 | 0.000 |
| Mo | 0.004 | 0.001 | 0.001 | 0.000 | 0.000 | 0.000 | 0.001 | 0.000 | 0.000 | 0.000 | 0.000 | 0.000 | 0.000 | 0.000 |
| Sn | 0.006 | 0.001 | 0.000 | 0.000 | 0.000 | 0.000 | 0.000 | 0.000 | 0.000 | 0.000 | 0.003 | 0.000 | 0.000 | 0.000 |
| Sb | 0.005 | 0.001 | 0.000 | 0.000 | 0.000 | 0.000 | 0.001 | 0.000 | 0.000 | 0.000 | 0.000 | 0.000 | 0.000 | 0.000 |
| Ba | 0.025 | 0.003 | 0.002 | 0.000 | 0.000 | 0.000 | 0.006 | 0.000 | 0.001 | 0.000 | 0.000 | 0.000 | 0.000 | 0.000 |
| Pb | 0.001 | 0.000 | 0.002 | 0.000 | 0.000 | 0.000 | 0.000 | 0.000 | 0.003 | 0.000 | 0.026 | 0.002 | 0.001 | 0.000 |
| Relative contribution | | | | | | | | | | | | | | |
| Element | Traffic | | Dust | | Sea/road salt | | Aged sea salt | | S-rich | | Solid fuel | | Reacted Cl | |
| | mean | std | mean | std | mean | std | mean | std | mean | std | mean | std | mean | std |
| Na | 0.000 | 0.000 | 0.000 | 0.000 | 0.240 | 0.003 | 0.760 | 0.003 | 0.000 | 0.000 | 0.000 | 0.000 | 0.000 | 0.000 |
| Mg | 0.048 | 0.005 | 0.058 | 0.004 | 0.143 | 0.007 | 0.635 | 0.011 | 0.019 | 0.002 | 0.054 | 0.004 | 0.044 | 0.004 |
| Al | 0.030 | 0.004 | 0.558 | 0.013 | 0.008 | 0.000 | 0.363 | 0.011 | 0.030 | 0.003 | 0.000 | 0.000 | 0.012 | 0.001 |
| Si | 0.062 | 0.006 | 0.752 | 0.011 | 0.008 | 0.000 | 0.016 | 0.000 | 0.042 | 0.003 | 0.109 | 0.008 | 0.011 | 0.001 |
| P | 0.193 | 0.018 | 0.130 | 0.010 | 0.074 | 0.004 | 0.005 | 0.000 | 0.192 | 0.015 | 0.306 | 0.019 | 0.100 | 0.009 |
| S | 0.000 | 0.000 | 0.001 | 0.000 | 0.029 | 0.002 | 0.000 | 0.000 | 0.652 | 0.009 | 0.318 | 0.010 | 0.000 | 0.000 |
| Cl | 0.000 | 0.000 | 0.000 | 0.000 | 0.406 | 0.009 | 0.000 | 0.000 | 0.000 | 0.000 | 0.000 | 0.000 | 0.594 | 0.009 |
| K | 0.000 | 0.000 | 0.000 | 0.000 | 0.032 | 0.003 | 0.125 | 0.007 | 0.001 | 0.000 | 0.820 | 0.010 | 0.022 | 0.003 |
| Ca | 0.027 | 0.005 | 0.852 | 0.010 | 0.046 | 0.004 | 0.072 | 0.004 | 0.003 | 0.000 | 0.000 | 0.000 | 0.000 | 0.000 |
| Ti | 0.188 | 0.032 | 0.603 | 0.040 | 0.000 | 0.000 | 0.000 | 0.000 | 0.007 | 0.001 | 0.202 | 0.026 | 0.000 | 0.000 |
| V | 0.432 | 0.041 | 0.216 | 0.024 | 0.000 | 0.000 | 0.000 | 0.000 | 0.071 | 0.010 | 0.239 | 0.028 | 0.042 | 0.006 |
| Cr | 0.673 | 0.037 | 0.318 | 0.037 | 0.000 | 0.000 | 0.009 | 0.001 | 0.000 | 0.000 | 0.000 | 0.000 | 0.000 | 0.000 |
| Mn | 0.366 | 0.043 | 0.399 | 0.039 | 0.037 | 0.004 | 0.028 | 0.002 | 0.000 | 0.000 | 0.170 | 0.022 | 0.000 | 0.000 |
| Fe | 0.736 | 0.016 | 0.216 | 0.016 | 0.000 | 0.000 | 0.000 | 0.000 | 0.004 | 0.001 | 0.042 | 0.004 | 0.001 | 0.000 |
| Ni | 0.256 | 0.037 | 0.197 | 0.025 | 0.331 | 0.028 | 0.000 | 0.000 | 0.056 | 0.009 | 0.160 | 0.022 | 0.000 | 0.000 |
| Cu | 0.690 | 0.032 | 0.230 | 0.028 | 0.007 | 0.001 | 0.011 | 0.001 | 0.000 | 0.000 | 0.057 | 0.008 | 0.005 | 0.001 |
| Zn | 0.095 | 0.019 | 0.209 | 0.027 | 0.000 | 0.000 | 0.000 | 0.000 | 0.012 | 0.002 | 0.684 | 0.035 | 0.000 | 0.000 |
| Br | 0.124 | 0.023 | 0.000 | 0.000 | 0.055 | 0.006 | 0.000 | 0.000 | 0.260 | 0.033 | 0.412 | 0.039 | 0.149 | 0.023 |
| Sr | 0.148 | 0.032 | 0.195 | 0.028 | 0.084 | 0.011 | 0.438 | 0.028 | 0.000 | 0.000 | 0.118 | 0.021 | 0.015 | 0.003 |
| Zr | 0.839 | 0.010 | 0.000 | 0.000 | 0.000 | 0.000 | 0.152 | 0.010 | 0.009 | 0.002 | 0.000 | 0.000 | 0.000 | 0.000 |
| Mo | 0.620 | 0.033 | 0.179 | 0.024 | 0.000 | 0.000 | 0.136 | 0.008 | 0.048 | 0.008 | 0.000 | 0.000 | 0.018 | 0.003 |
| Sn | 0.605 | 0.039 | 0.035 | 0.005 | 0.000 | 0.000 | 0.000 | 0.000 | 0.038 | 0.006 | 0.287 | 0.034 | 0.035 | 0.005 |
| Sb | 0.702 | 0.027 | 0.056 | 0.008 | 0.000 | 0.000 | 0.077 | 0.005 | 0.070 | 0.010 | 0.071 | 0.011 | 0.024 | 0.004 |
| Ba | 0.728 | 0.020 | 0.067 | 0.010 | 0.000 | 0.000 | 0.183 | 0.011 | 0.021 | 0.004 | 0.000 | 0.000 | 0.000 | 0.000 |
| Pb | 0.026 | 0.006 | 0.064 | 0.010 | 0.000 | 0.000 | 0.000 | 0.000 | 0.096 | 0.016 | 0.781 | 0.027 | 0.034 | 0.006 |

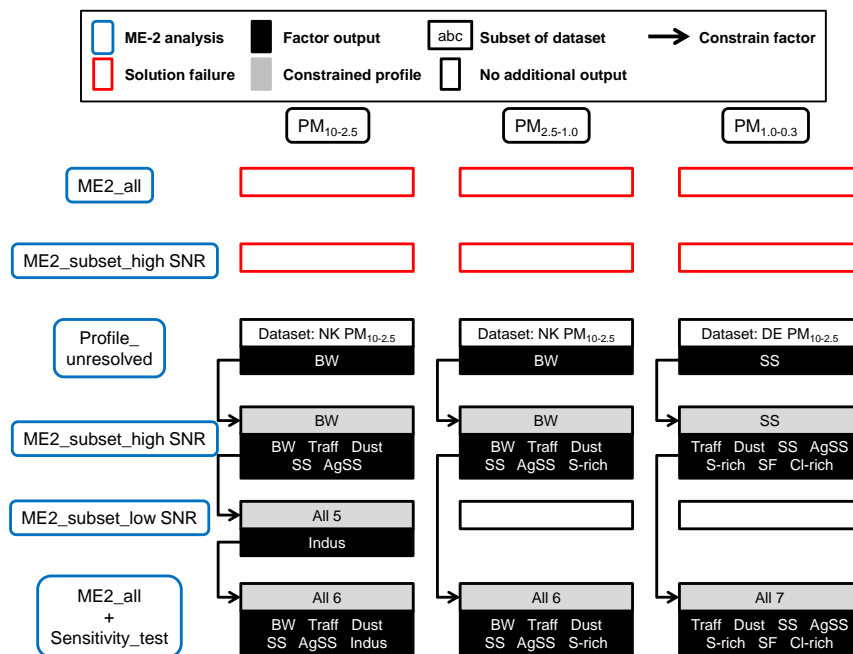


Figure 5. ME-2 analysis strategy for $PM_{10-2.5}$, $PM_{2.5-1.0}$ and $PM_{1.0-0.3}$ on MR-NK-DE sites combined (see Fig. 2 for explanation of blue boxes). MR: Marylebone Road, kerbside; NK: North Kensington, urban background; DE: Detling, rural site. Each step is followed by ME2_all, but always failed except in the last step. Input profiles are constrained with a value = 0.1. The model runs were performed on 3–10 factors and 10–20 seeds to explore local minima in the solution space to find those that are most meaningful. Sources: BW: brake wear; Traff: other traffic-related; Dust: resuspended dust; SS: sea/road salt; AgSS: aged sea salt; Indus: industrial; S-rich: S-rich; SF: solid fuel; Cl-rich: reacted Cl. See Sect. 2.3 for more details.

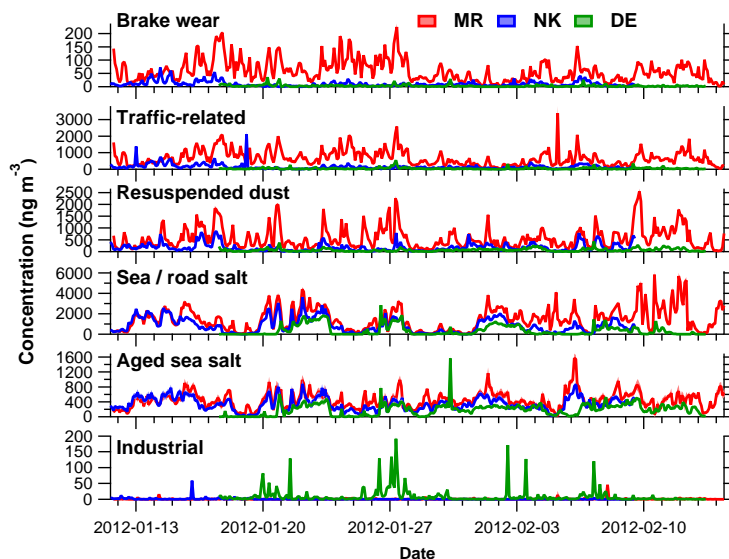


Figure 6. $PM_{10-2.5}$ source contributions (factor time series) according to the ME-2 analysis on combined data of the three sites (MR - Marylebone Road, kerbside; NK - North Kensington, urban background; DE - Detling, rural). Data is given as mean ± 1 standard deviation (shaded area) from the anchor sensitivity analysis.

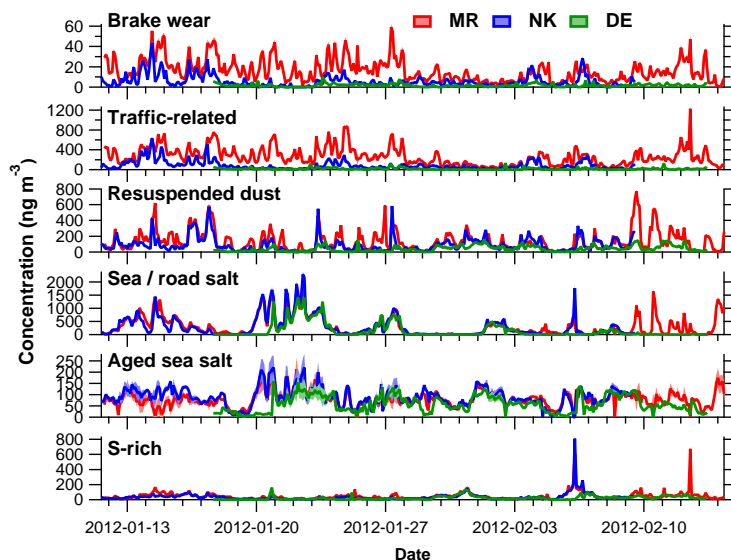


Figure 7. $PM_{2.5-1.0}$ source contributions (factor time series) according to the ME-2 analysis on combined data of the three sites (MR - Marylebone Road, kerbside; NK - North Kensington, urban background; DE - Detling, rural). Data is given as mean \pm 1 standard deviation (shaded area) from the anchor sensitivity analysis.

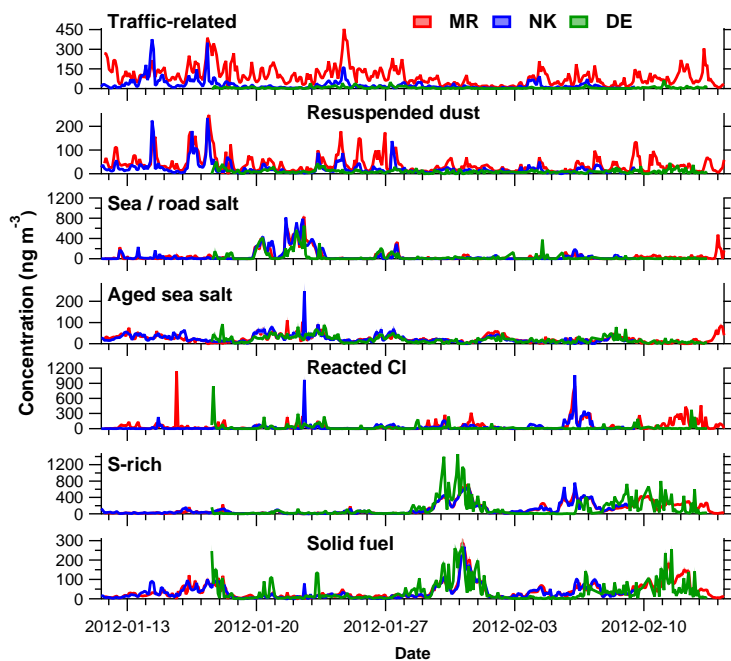


Figure 8. $PM_{1.0-0.3}$ source contributions (factor time series) according to the ME-2 analysis on combined data of the three sites (MR - Marylebone Road, kerbside; NK - North Kensington, urban background; DE - Detling, rural). Data is given as mean \pm 1 standard deviation (shaded area) from the anchor sensitivity analysis.

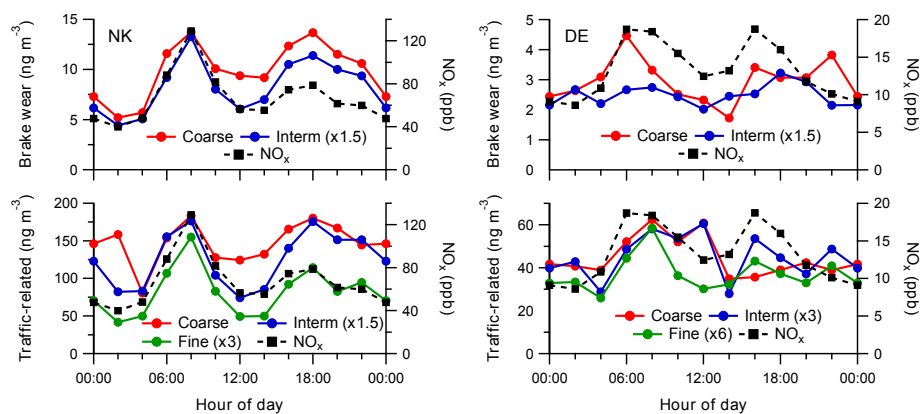


Figure 9. Diurnal variations of the brake wear ($PM_{10-2.5}$ - coarse, $PM_{2.5-1.0}$ - interm) and other traffic-related (coarse, interm, $PM_{1.0-0.3}$ - fine) factors at NK (left) and DE (right) compared to diurnal variations of NO_x . Hour of day is start of a 2 h sampling period (00:00 UTC means sampling from 00:00 to 02:00 UTC). Note the scaling applied to several tracers.

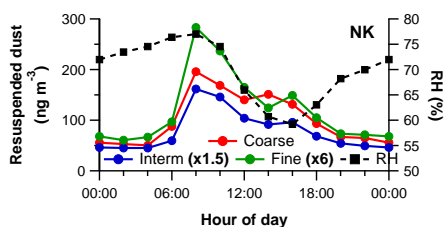


Figure 10. Diurnal variations of the resuspended dust ($PM_{10-2.5}$ - coarse, $PM_{2.5-1.0}$ - interm, $PM_{1.0-0.3}$ - fine) factors at NK compared to the diurnal variation of relative humidity (RH). Hour of day is start of a 2 h sampling period (00:00 UTC means sampling from 00:00 to 02:00 UTC). Note the scaling applied to several tracers.

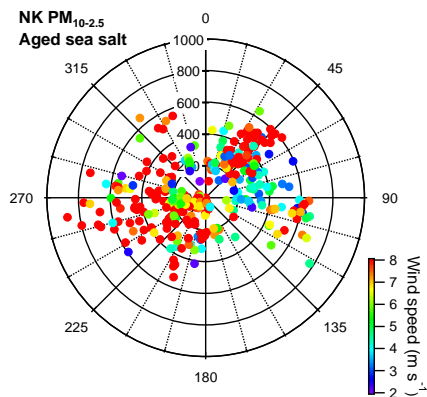


Figure 11. Wind rose of the aged sea salt factor at North Kensington for $PM_{10-2.5}$ ($ng\ m^{-3}$), color-coded by the wind speed. Data points with wind speed $< 2\ m\ s^{-1}$ are ignored. Wind roses are similar at Marylebone Road and Detling.

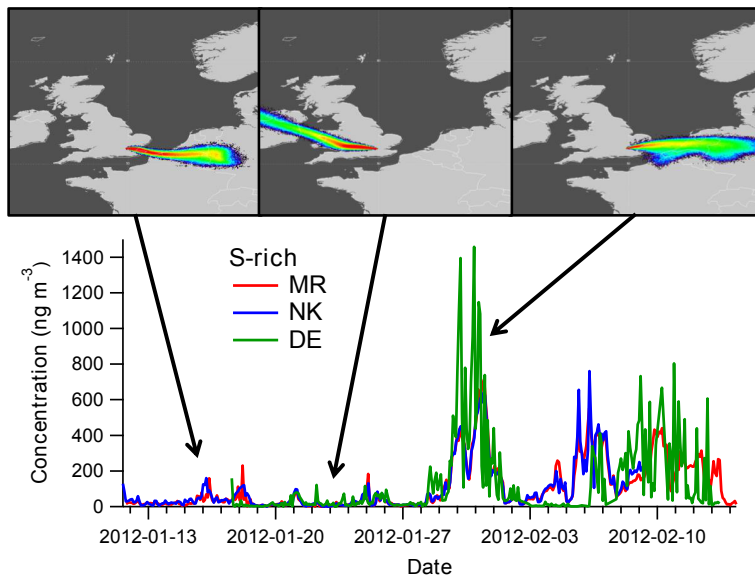


Figure 12. Time series of the S-rich factor in $\text{PM}_{1.0-0.3}$ at MR, NK and DE. The three footprints are simulated with the NAME model for particles released from the BT Tower and followed back at 0–100 m, a.g.l for the previous 24 h; particle concentrations increase from blue to red. Periods with high S-rich concentrations correspond to footprints from northern Europe (left and right), whereas low S-rich concentrations correspond to footprints from e.g. the west (centre).

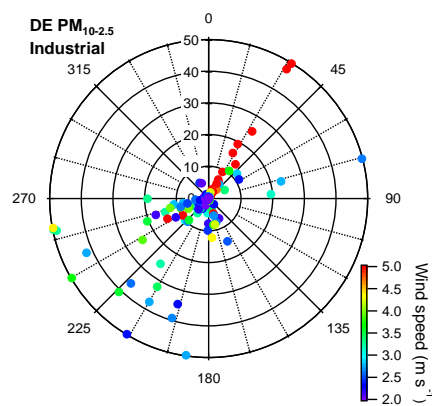


Figure 13. Wind rose of the industrial factor at DE for $\text{PM}_{10-2.5}$ (ng m^{-3}), color-coded by the wind speed. Data points with wind speed $< 2 \text{ m s}^{-1}$ are ignored. Note that data points $\geq 50 \text{ ng m}^{-3}$ are set to 50 ng m^{-3} to improve visualisation.